Factors in Life Testing Ion Engines

J. R. ANDERSON,* S. A. THOMPSON,† AND H. J. KING‡
Hughes Research Laboratories, Malibu, Calif.

The goal of contemporary ion rocket research and development is the attainment of reliable, long-life ($\geqslant$10,000 hr) operation. In addition to vacuum test chamber environment, the interaction of electrode thermal characteristics and neutral efflux from the ionizer are dominant in determining surface-contact ion engine lifetime. Several key physical processes are discussed in the light of recent experimental results. Charge exchange erosion is the fundamental limitation to engine lifetime. Although experiment and analysis indicate attainable lifetimes of 5000 to 20,000 hr at 10 ma/cm² using the "best" present-day ionizers, shorter lifetimes result when interrelated secondary physical phenomena within the acceleration region of the engine emerge. Cesium ionization on the focus electrodes is considered in detail, since it is a lifetime barrier in those designs which utilize such beam-forming elements. Tolerable charge exchange erosion of accel electrodes, to assure a given lifetime, is used to provide boundary conditions for ionization efficiency, focus temperature, and focus ion current. The effect of focus electrode roughness on accel erosion patterns is studied in detail. The influence of the ground-based test chamber environment vs a true space vacuum environment is also considered.

Fundamental Limitations to Thruster Lifetime

FUNDAMENTAL limitations to surface-contact ion engine lifetime are 1) additional sintering of the porous tungsten ionizer, 2) tungsten evaporation, 3) neutralizer life, and 4) ion erosion of the accel electrode.

Preliminary experimental data[1] indicate that, at most, a 3- to 5-μ tungsten powder, sintered between 80 and 82% theoretical maximum density, would undergo a density increase of only 2% in one year at 1200°C, a temperature substantially above those required to produce cesium ion current densities up to approximately 40 ma/cm² with a clean ionizer. The 2% density increase would decrease the permeability through the porous ionizer by about 33%. In the case of cesium originally at a source pressure of 1 torr, the decrease in permeability can be compensated by increasing the cesium temperature by approximately 15°K, which would be well within the range of any practical control system.

Tungsten can be transported to the gas phase in the form of a molecular compound in the presence of oxygen or water vapor. This problem is significant when the oxygen partial pressure results in appreciable evaporation of WO_3.[2] An oxygen partial pressure of 10^{-8} torr would result in a tungsten loss of 2×10^{-4} g/cm²/yr, or 1.6×10^{-5} cm/yr from the surface of a 70% theoretical density ionizer. Conditions inside a vacuum chamber could be troublesome, but the loss of tungsten by evaporation in outer space is insignificant. However, some evaporated tungsten oxide condenses onto accel electrodes. When covered with cesium, the oxide coating can have a low work function surface and correspondingly high electron emission. In addition, loosely adhering metallic deposits on accel electrodes have been identified as tungsten. Such flakes lead to voltage breakdown in the accelerating portion of the thrustor.

Neutralizers not subject to ion bombardment can have lifetimes that are long as compared with other engine components. Ions striking the filaments sputter the active ingredient (e.g., thorium) off the surface and ultimately destroy physical continuity. Carburization reduces thorium evaporation and inhibits deactivation resulting from ion bombardment.[3,4] A filament 0.015 in. in diameter, 50% carburized, would last over 10,000 hr at an electron emission of 500 ma (4.12 amp/cm²).[5] The end-of-life criterion used is filament decarburization in a power tube environment. Since decarburization is expected to be negligible in space, in the absence of oxygen, thorium evaporation and ion bombardment should become the limiting factors. They can also lead to contamination of the ionizer with filament constituents that will plug pores or alter the work function. This is accentuated by the fact that better coupling of the neutralizer to the beam is achieved the closer it is moved toward the exit aperture, where it can also "see" the ionizer better.§

Because ionization efficiency is not ideally 100%, cesium atoms are present in the accelerating region, and resonant charge exchange collisions occur. Many charge exchange ions created in this region are attracted to the accel electrode, causing erosion and eventual destruction. The extent of this erosion depends on the reaction length, the capability to focus charge exchange ions out of the engine, the accelerator material, and the neutral fraction. Because of space charge and voltage breakdown limitations, the reaction length cannot be made arbitrarily short. No accelerator system appears to be capable of simultaneously extracting a beam and focusing all charge exchange ions out of the engine. Also, because of diverse requirements, accel electrodes are generally copper, which has a high sputtering yield. Other materials, such as beryllium, show promise for reducing sputtering yield while satisfying other accel requirements. Until they are proved, the best method for limiting charge exchange erosion is to reduce the neutral efflux from the ionizer.[7] The importance of this reduction can be seen in Fig. 1, which relates ionizer current density to operating life for the Hughes Model 70 ion optics in a linear strip geometry. End-of-life occurs when a portion (area A in Fig. 1) of the accel electrode is eroded away. It is assumed that areas of the accel critical to the optics are relatively unaffected.

The neutral efflux has a strong effect on life. At a neutral fraction of 5%, a life of 1 yr can be achieved at a maximum current density of 7 ma/cm². Reducing the neutral fraction to 1% allows the current density to increase to 15.7 ma/cm² for 1 yr, or the life to increase to 5 yr at 7 ma/cm².

Presented as Preprint 64-685 at the AIAA Fourth Electric Propulsion Conference, Philadelphia, Pa., August 31–September 2, 1964; revision received April 23, 1965. The authors would like to acknowledge the fine technical support of P. J. Coane, without whose aid much of the experimental data would not have been obtained.

* Senior Member of Technical Staff.
† Member of Technical Staff.
‡ Member of Technical Staff. Member AIAA.

§ For details of an approach to the design of contact ion engines for long life, the reader is referred to a companion paper.[6]

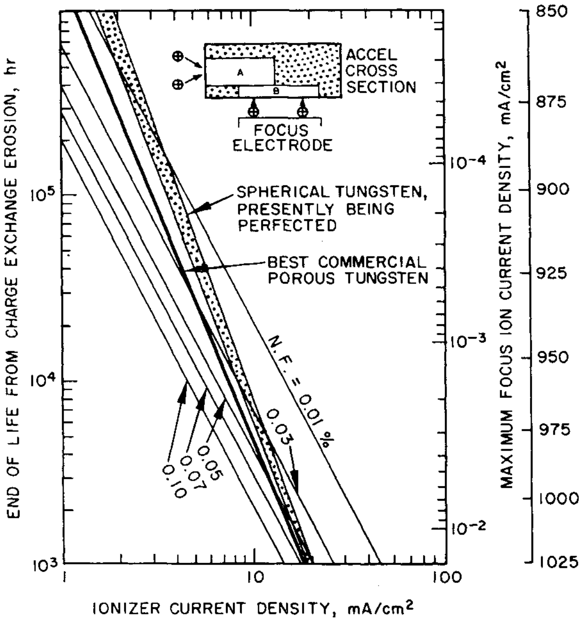

Fig. 1 Effect of charge exchange ions on cesium contact ion engine lifetime. Accel-ionizer voltage = 10 kv, copper accel and copper-coated focus electrode, and linear multistrip geometry. End of life by charge exchange erosion occurs when area A is sputtered away, and allowable erosion by focus electrode ions is area B.

Direct bombardment of the accel by ions generated at the ionizer can be maintained to less than one particle in 10^5, and, in fact, with present-day knowledge and techniques of accelerator design, there should be no excuse for observing direct impingement of ions from any place on the ionizer onto the accelerator electrode.[8] Thus, we reach the conclusion that charge exchange erosion of the accel electrodes is the fundamental limit to thruster life.

Secondary Limitations to Thruster Lifetime

Lifetimes shorter than predicted by charge exchange analysis occur because of the emergence of secondary physical phenomena, usually within the accelerating region of the engine. Methods have been and are being developed to suppress the effects of these phenomena so that the charge exchange lifetime limit can be reached. The principal secondary problems that have been encountered are 1) focus ionization, 2) time-dependent drains from the accel electrodes, and 3) environmental limitations in ground-based vacuum chambers.

Interdependence of Electronic and Thermal Effects

Before treating these secondary limitations in detail, it should be stressed that the various components of drain currents between the accel and focus electrodes are interdependent. The relation between electrode temperatures, neutral efflux, and electron and ion emission has been studied analytically, and a graphical method for illustrating this interdependence and predicting stable engine operating points has been developed.

The accelerator drain current results from both electron emission and ion collection by this electrode. It is imperative to minimize the ion component of drain current in order to reduce the sputtering damage. Electron current leaving the accel heats the focus and ionizer electrodes but does no serious physical damage. Heating the ionizer by electron bombardment merely reduces the heater power requirement. Increasing focus temperature is undesirable, since the ion emission density that this electrode is capable of supporting increases with temperature. Thus, the heat input to the focus electrode must be limited to that which can be rejected without appreciably raising the temperature.

The complexity increases in thrusters composed of an array of linear ion emitters, because there is a temperature gradient along each electrode and the thermal environment at the periphery differs considerably from the center. To illustrate the interdependence of the phenomena, we shall consider a general case and attempt to isolate critical areas and investigate any regions of instability. First, we must know the electron and ion emission from the accelerator and focus electrodes, respectively, as functions of temperature, as well as their temperature profiles as functions of radiant and electrical input power.

Many critical temperature curves for ion emission are available,[9] as are some S curves for electron emission.[10] Temperature profiles can be calculated for a specific thruster design. The latter two statements assume that the surface characteristics and emissivities of the electrodes are known and remain constant. In practice, this is not necessarily true, and a series of solutions of the type outlined below is found which covers a range of these variables and can then be compared with experimental data.

None of the required functions can be expressed in concise mathematical form, and so graphical techniques must be employed, as shown in Fig. 2. This composite graph includes the characteristics representing power vs temperature and current vs temperature of the focus and accelerating electrodes for a linear strip geometry. Plotted in the upper left corner is the ion emission from the focus electrode as a function of maximum focus temperature. The ions so created will be attracted to the accel electrode with a potential drop on the order of 10 kv and will increase the temperature as shown in the upper right graph. This accel electrode temperature will result in thermionic electron emission, as given in the graph at lower right. That fraction of the electrons from the accel electrode passing to the focus electrode, combined with the heat that the focus electrode receives from the ionizer by

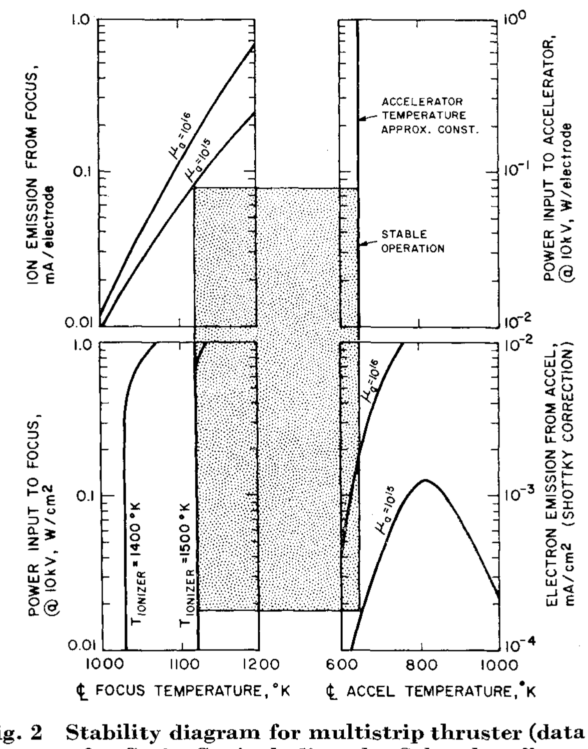

Fig. 2 Stability diagram for multistrip thruster (data on S-curves for Cu in Ce, including the Schottky effect correction are courtesy of R. G. Wilson, Hughes Research Laboratories). Focus electrodes: molybdenum, 8 cm long; accel electrodes: copper, 10 cm long; current density: 15 ma/cm².

radiation, results in the peak focus electrode temperature indicated in the lower left graph. The shape of each of these graphs is, of course, determined by the thermal characteristics (power inputs, thermal conductance, etc.). The operating point must be self-consistent among these four graphs if the operation is to be stable.

Several general features of the solutions are of importance:

1) An operating point to the right of the peak on the S-curve (lower right, Fig. 2) is stable, since increasing accelerator temperature reduces the electron emission and subsequently the power input to both the focus and accelerator electrodes.

2) Operation to the left of the peak is stable only if the initial operating point is such that the electrical power to the electrodes is small compared with the radiant power (i.e., the thermal impedance between the electrode and heat sink is small). A large transient (arc, propellant surge, etc.) may shift the operating point sufficiently so that it will be necessary to shut off the ion beam to re-establish the original operating point.

3) Ion emission from the focus electrode will be limited by the electrode temperature and not by the neutral efflux, which is far too high in present ionizers.

4) The accelerator temperature plays a major role in defining the operating point and stability. This temperature is directly determined by the heat rejection path and heat input for a particular design.

From the preceding discussion, it is apparent that the input data, particularly S curves for copper with an adsorbed oxygen layer, are not sufficiently accurate to predict quantitatively the exact stability points. However, even semiquantitative information is of considerable value in evaluating thrustor designs.

Observe also the effect of increasing the accelerator temperature so that operation is at a minimum on the S curves. The total drain current decreases; however, the ion component, which causes erosion, increases because of increased focus temperature. The increased focus temperature in this case reflects the fact that the reduction in electrical power to the focus (due to reduced electron emission) is more than compensated by an increase in radiant power due to the increased accel temperature. Using such a diagram, it is possible to establish a minimum ion emission current as a function of accelerator temperature for any specific design. The ability to investigate such parameters makes this analog technique very valuable.

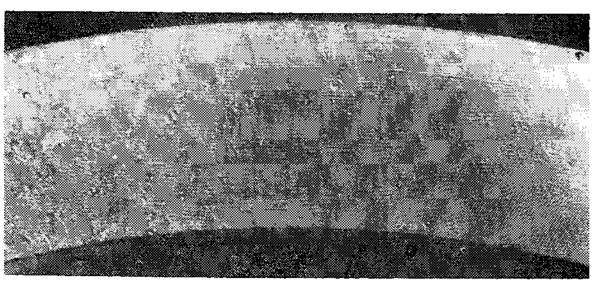

a) Focus electrode.

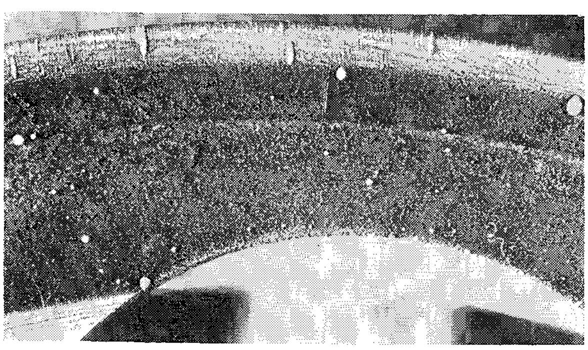

b) Opposing area on accel electrode.

Fig. 3 Opposing surfaces of focus and accel electrodes after an 80-hr test in an annular cesium ion engine.

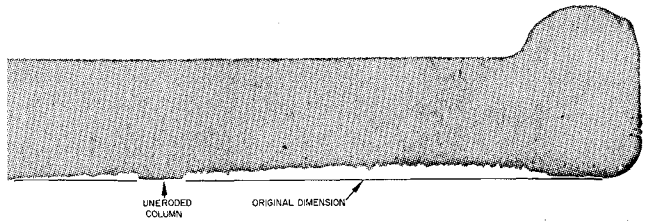

Fig. 4 Cross section of the accel electrode shown in Fig. 3 (30×).

Ionization on Focus Electrodes

Cesium adsorbing on the focus electrodes can ionize by surface contact and be attracted to the accel electrodes. There is a maximum accel volume (region B in Fig. 1) that can be eroded if area A is reserved for charge exchange erosion. The maximum allowable focus ion current density is directly proportional to lifetime and is plotted on the right-hand ordinate along with the associated focus electrode critical temperature. Critical temperature is used, since, in practical thrusters, the arrival rate of cesium atoms always exceeds the tolerable current density.

Accel erosion patterns resulting from ionization at the focus electrode have been studied in detail. The erosion patterns can be shown to originate at the surface of the focus electrodes. Figure 3 shows opposing areas of a focus (Fig. 3a) and an accel electrode (Fig. 3b) that operated for 80 hr in an annular ion engine with relatively high ionization of neutral cesium on the focus electrode surface. The focus electrode photograph has been reversed for this comparison. The dark area on the accel is the area oposite the focus. Note the regularly spaced ridges and valleys on the accel electrode and the white dots interspersed throughout the heavily eroded area. Figure 4 is a 30× picture of a cross section of the same accel electrode. The eroded area has a regular jagged appearance. The protrusion designated as an uneroded column corresponds to a white dot in Fig. 3b. The bases of these columns usually have been more severely eroded than other areas. Figure 5 is a 330× picture of the column. The coating over its top is stainless steel sputtered from other parts of the accel or reflected from the focus electrode. The stress marks along the top of the column, which resulted from machining, rule out the possibility that the column originated during operation of the thruster.

A model that explains patterns on the accel can be formulated by considering the formation of a column. In Fig. 3a there are small peaks on the focus opposite each accel column. These peaks are bits of hard substances imbedded in the sur-

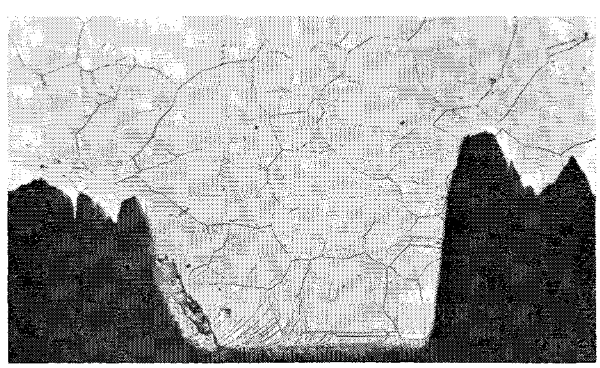

Fig. 5 Cross section of the column shown in Fig. 4 (330×).

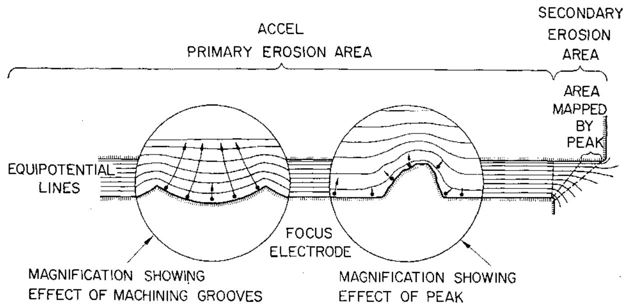

Fig. 6 Equipotential diagram in regions of peaks and valleys on the surface of the focus electrode. The resultant perturbation of the initial ion trajectories is shown in the magnified views.

face of the focus electrode. Macroscopically, the equipotentials in the accel-focus electrode gap are parallel to the electrode surfaces between electrodes, but microscopically, equipotential lines near the surface are distorted by peaks or valleys on the focus surface (Fig. 6). Ions created on or very near a peak have a horizontal component to their initial velocity, since they follow the lines of force, which are perpendicular to the equipotentials. These ions do not strike the accel opposite their point of origin, and an uneroded column is left standing opposite a peak on the focus. Many diverted ions impact next to the column, adding to the normal erosion at the base of columns. Toward the outer edge of the focus electrode, the fields are such that peaks map into elongated areas on the accel, and the results are oblong "mesas," some of which can be seen in Fig. 3b.

Figure 6 also illustrates how the electric field near the surface of the focus electrode tends to focus ions into specific areas near the center of each machining groove. This is responsible for the pattern of erosion ridges on the accel in Figs. 3 and 4. The pattern is altered in areas of extensive erosion because sputtered accel material obscures the focus machining grooves, and ion focusing becomes less sharp. In those areas, the accel peaks become shorter, more rounded, and more randomly located. This is also true opposite focus electrodes that have ground or lapped finishes.

Most of the columns produced on the accel are very thin, and as the accel is sputtered away around them they stand taller and become excellent sources of field-enhanced electron emission, which increases the accel drain current. For an isolated peak with a height five times its base radius (roughly the ratio for peaks on the accel in question), the field enhancement factor at the peak is 7.5. This figure applies for a peak that has no other peaks within a distance of twice its height[11]; allowing for bunching, the enhancement may be arbitrarily reduced by a factor of 2. For the case of $T = 700°K$ and an applied voltage of 10 kv, the electric field enhancement becomes significant if the peak height to base radius is 8.5. For this case, the electric field strength is enhanced by a factor of 28, and the Schottky term in the electron emission relation increases by a factor exceeding 1000. Many of the columns approach these height/base-radius ratios; fortunately, their total emitting area is small. Proper conditioning (e.g., electropolishing) of the focus electrode surface prior to engine operation can eliminate column formation.

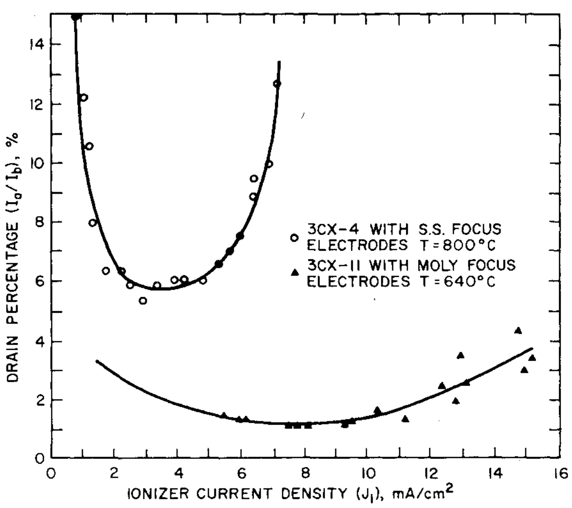

Fig. 7 Percentage accel drain as a function of ionizer current density for two different focus electrode materials.

There are several methods for suppressing focus ions: reducing the focus temperature, cesium arrival rate, or surface work function; rasing the critical temperature; or designing electrodes to focus the ions out of the engine. At present, only reduction of focus electrode temperature has yielded positive results. Order-of-magnitude improvement has been demonstrated with this technique. An example of the decreased drain current that can result from decreasing focus electrode temperature (if initially too hot) can be seen in Fig. 7.

Time-Dependent Accel Drain Current

A phenomenon that has been encountered in contact and electron bombardment engines using cesium is the increase of accel drains with time. At a certain point in time, the accel current becomes unstable and increases rapidly to relatively high levels. The cause of this phenomenon has been postulated to be an adiabatic change in the surface state of the accel electrode, such as adsorption and/or nucleation of cesium and oxygen on the accel, resulting in a lowered work function and field-enhanced electron emission. Heating the accels has been shown to lower drain currents substantially, perhaps because some oxygen desorbs from the surface. Insufficient experimental data have been gathered to establish the acceptable temperature bounds, although preliminary data for cesium on copper indicate that the temperature range of 600° to 1000°K may be unfavorable.[12]

Environmental Considerations

Since thruster testing and evaluation can only be conducted in a vacuum environment, preferably with a pressure less than 10^{-6} torr, test chambers must be equipped to insure a low background pressure of engine propellant, oxygen, water vapor, and particularly carbon-bearing gases.

A difficult space characteristic to simulate in a ground-based test chamber is the electric environment. The electric potential and fields in the exhaust beam from an ion engine in space will be determined by the charge distribution in the beam and by the boundary condition imposed by the spacecraft. In the ground-based vacuum chamber, the surrounding metallic walls and beam collector impose highly artificial electrical boundary conditions around the beam, as shown in Fig. 8.

It is difficult to isolate, to a degree comparable with the electrically isolated space vehicle, the experimental engine in a ground-based test. In the absence of suitable isolation, the effects of a slight unbalance in electron and ion emission may not be detectable in ground tests, whereas such charge unbalance could be detected readily on a space vehicle. Correlation between ground and space performance of the SERT-I ion engine has shown the basic validity of ground-based neutralization experiments[13–16] and has given confidence that the neutralization of an ion beam in space presents no significant problem. However, the absence of any long-term effects can be verified only by life tests in the real space environment, such as would be provided by an orbiting ion engine.

Gaseous contaminants

Referring again to Fig. 8, note that the artificial vacuum created in ground-based chambers is subject to the presence of undesirable residual vapors. Among the potential contaminating gases, oxygen (either in atomic or molecular form) and the carbon-bearing molecules are the most serious. Oxygen adsorbed onto the porous tungsten ionizer will increase the work function and so decrease the neutral cesium efflux to a value not simulating operation in space. Thus charge-exchange life-time as determined in test chambers could be too optimistic. Calculations[17] of the effect of oxygen on tungsten ionizer performance show that an arrival rate of 7×10^{12} atoms/cm^2-sec, correspondng to a partial pressure of 2×10^{-8} torr, will increase the work function by approximately 0.3 ev and decrease the neutral efflux by a factor of about 10 for an ionizer current density of 12 ma/cm^2 and a temperature of 1500°K. Thus the oxygen partial pressure in the chamber should be maintained as much below 10^{-8} torr as possible.

Carbon-bearing gases, possibly orginating in the oil diffusion pumps, produce lower work functions and high neutral fractions initially, while still requiring a higher critical temperature. The probability of a carbon atom sticking to the tungsten surface has been measured[18] to be roughly 1 to 2×10^{-3} for 10 of the more common carbon-containing molecules. The carbon diffuses into the outer tungsten grains, leaving a relatively low surface coverage of carbon. As the carbon content of the grains increases, the diffusion rate is reduced, and the surface concentration increases. Figure 9 gives the surface coverage of carbon on an ionizer, for a given operating time, as a function of the partial pressures of the four carbonaceous gases most likely to be found in a typical vacuum system.[19] Even low surface coverages of carbon (left scale), which evolve at low partial pressures of carbonaceous gases (bottom scales), significantly lower the ionizer work function (right scale); e.g., a 1% carbon coverage reduces ϕ from 4.54 to 4.27 ev after 500 hr at a partial pressure of 5×10^{-7} torr for CO alone. If CO, CO_2, and CH_4 have partial pressures of 10^{-8} torr each, the total effect is a 0.4% carbon coverage and a work function of 4.4 ev after 500 hr. At 10% carbon coverage, a work function of 2.97 ev is reached. Further increase in carbon coverage would cause the work function to rise; when a pure carbon (graphite) surface evolves, the work function increases to a stable value of 4.62 ev, but the graphite surface is not favorable because of the increased critical temperatures required for ionization of cesium.[20]

Collector sputtering

A collector system should collect the beam, direct as much expended propellant as possible to the cryowalls, protect the chamber from sputtering damage, and minimize sputtered material to the engine area. The foremost problem is backsputtering onto the engine. Typical collectors are made of copper because it can be vaporized readily from the ionizer and does not affect ionizer performance at copper arrival rates below 10^{14} atoms/cm^2-sec. Vaporized copper deposits on electrodes may flake off during temperature cycling, thereby causing interelectrode shorts. Reducing the incidence of copper to the engine can be accomplished by geometric changes in the collector or reduction of ion impact energies.

The collector should be as remote as practical to take advantage of $1/r^2$ reduction of the solid angle subtended by the engine. The possibility of reducing copper incident on the engine by directing the beam to the collector at a shallow grazing angle is dependent on sputtering yield and distribution. The yield of sputtered material increases as the cosine^{-1} of the incident angle up to about 70° from the normal.[21,22] Since the arrival rate at the ionizer decreases as the cosine of the incident angle, no benefit is derived at collector angles up to 70°. If very shallow grazing angles are used (above 75° to the normal), the arrival rate decreases because the sputtering yield levels off and decreases as the incident angle increases further.[22]

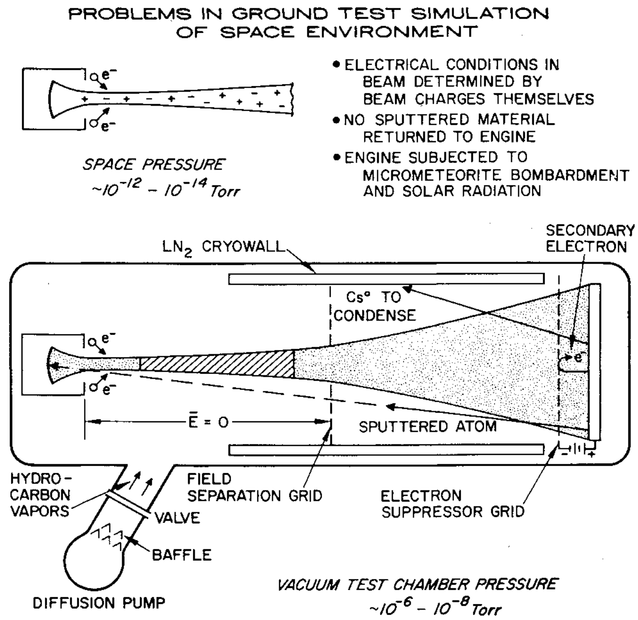

Fig. 8 General features of the envirnoment which are important to operation of ion engines in space and ground-based test chambers.

Future engines, operating at much higher currents, present a problem. At normal ionizer temperatures, an arrival rate of copper above 10^{14} atoms/cm^2-sec exceeds the vaporization rate, and copper begins to build up on the ionizer. The process is enhanced by charge-exchange sputtering and copper accel electrodes. There is a decrease in ionization efficiency, and plugging of some pores may ensue. An engine may have to stop thrusting repeatedly to vaporize excess copper so that life testing may continue. Vaporized copper would plate out on electrodes and could change engine optics and/or cause electrical breakdown.

Decelerating the beam to reduce the yield/ion, or deflecting the beam so that it sputters in a harmless area, is a possible solution, but neither has been proved. An additional advantage to beam deceleration would be a more favorable

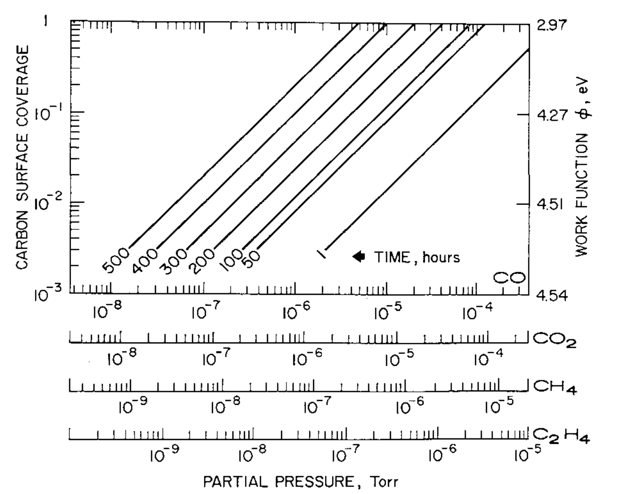

Fig. 9 Surface coverage of carbon and work function of a porous tungsten ionizer as a function of the partial pressures of four common carbon-bearing residual gases found in oil-diffusion-pumped vacuum chambers. These empirical calculations are valid for a 5-μ tungsten grain ionizer at 1600°K.

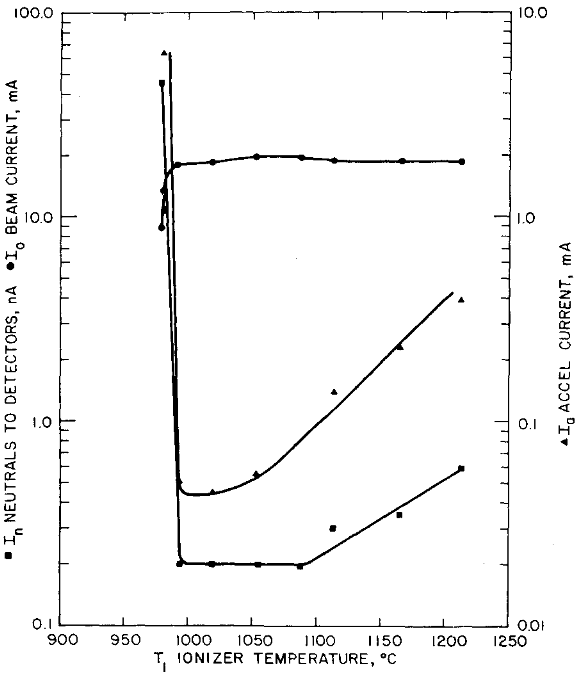

Fig. 10 Typical curves of neutral flux, accel current, and beam current as a function of ionizer temperature for an annular ion engine.

distribution of sputtered material about the reflected angle instead of about the normal at the lower impact energies.[22,23] Deceleration must be almost complete to achieve very large yield reductions because of the slow decrease in yield with decreasing energy[24] at normal operating voltages.

The amount of total copper eroded is not trivial for large engines. For example, a 30-kw engine will sputter over 100 lb of copper in 800 hr. As the collector surface is roughened by erosion and/or the collector plates sputter to each other the net amount of copper to the engine remains constant, but the net loss from the collector is reduced somewhat.

A Thruster Control to Optimize Lifetime

Control loops must be developed to stabilize and optimize thrustor performance if long-lived ion engines are to become a practical reality. Such controls are desirable for the following reasons: 1) excess heater or drain power requires larger power supplies; 2) excess neutral flux implies additional propellant must be aboard; 3) destructive drain currents limit engine and mission life; and 4) variations in beam power can result in navigational problems. A detailed analysis has been carried out for a complete control system,[25] but this paper will restrict discussion to a phenomenon that merits attention for possible application in a control loop during thruster life tests.

Maximizing engine life is directly related to minimizing neutral flux, since charge exchange ion erosion is the fundamental limit. Figure 10 shows a typical plot of beam current, accel current, and neutral detector current vs ionizer temperature as measured on an annular ion engine. Details of the bottom of the neutral flux curve are obscured because the neutral detector was operating close to its background reading. Experiment shows that accel current minimizes at the same ionizer temperature as neutral flux, so that accel current is eligible for controlling ionizer heater power and neutral efflux. The attractivess of such a system is the elimination of a complex neutral detector in favor of an existing accel electrode.

Another advantage of control around the minimum point in the accel current-ionizer temperature characteristic is that the minimum total power point is only a few degrees below the minimum neutral flux-accel current point. As ionizer power is reduced past the drain minimum, the rise in accel current is so steep that the increase in accel power offsets any saving in ionizer power. The minimum accel drain current point thus becomes a multiple optimization point for ionization efficiency, accel drain current, and total power. A prototype control loop, embodying the principle of seeking

Table 1 Space and ground tests of thruster

Feature evaluated	Ground test	Unmanned space test: Short time (1 hr)	Unmanned space test: Long time (1 to 6 months)
Thrust	Direct-reaction measurement, can be calculated from measured V_f and I_b	Change spin rate linear acceleration, reaction wheel	Change in orbit
Electrode drain currents	Direct measurement of current influenced by chamber environment	Current measurement with data telemetered to ground, less contamination, due to environment	
Electrode erosion	Electrode weight change, sputtered material weight, visual inspection	Insufficient time for erosion test	Sputtered material weight, visual inspection by engine recovery, engine perveance change
Ionizer emission	Direct emission and neutral efflux measurement, vacuum preferably 10^{-8} torr	Emission data, vacuum to 10^{-12} or better	Emission and neutral efflux data, vacuum limited only by vehicle, long-duration test of surface and cesium contaminants
Long-duration reliability test	Life tests in vacuum chamber with solar simulation possible, failure mode analysis possible	Insufficient time for real reliability test	Most realistic test of system reliability, engine in real operating environment
Neutralization net vehicle charge	Measure net engine current isolated engine test, electrometer	Electric field meter, change in thrust with vehicle charge, isolated system except for plasma in space	
Beam-charge neutralization	Movable beam sampling probes, charge induction pulse test, electron beam probe	Fixed beam sampling probes, can test in real electrical environment (isolated)	Fixed beam sampling probes, real electrical environment, lower charged-particle density (background)
Arcing damage and protection	Direct measurement and observation, degree of damage determined easily	Better vacuum and lower propellant background pressure	Micrometeorites can cause arcs
Ionizer sintering	Direct measurement of porosity and density vs life	Not applicable, insufficient time	Better vacuum can possibly reduce sintering rate, only indirectly (flow) measurable

the accel drain minimum, has been tested and its feasibility proved.

It should be noted that the operation of such a system depends on accel temperatures being on the left side of the S-curves (Fig. 2), so that reducing accel temperature and cesium arrival rate (by reducing ionizer temperature) reduces drains, but reducing ionizer temperature too far increases neutral flux so much that drains increase from that point on. These phenomena give the accel current its minimum. The system will not work on a thruster having a hot copper accel, because, once the ionizer temperature starts to rise, accel current always diminishes, and the system runs away until maximum ionizer power or a melted accel electrode results.

Conclusions

The fundamental limit to cesium contact engine life is charge-exchange erosion of the accel electrode. Reducing the neutral particle efflux from the ion source is presently the only practical method for reducing the effects of this phenomenon.

Focus electrode ionization and time-dependent accel drain current increase are primarily responsible for thruster failures prior to reaching charge-exchange limitations. Because of the interdependence of drain currents, electrode temperatures, and neutral flux, these problems cannot be treated independently. Graphs indicating engine stability can be constructed to aid in accounting for the effects of this interdependence.

Erosion patterns on the accel electrode resulting from focus ion bombardment originate at corresponding surface patterns on the focus electrode. A logic network to control ionizer heater power can be constructed to eliminate the requirement of a neutral detector and optimize ionization efficiency, drain current, and total power simultaneously by utilizing the accel current vs ionizer temperature (or power) characteristic.

A realistic program for the development of electrical propulsion systems must include a series of flight tests for evaluation of component and system performance in the real space environment. Such expensive tests require that extensive life tests in ground-based chambers precede long-term space tests. However, in certain technical areas, ground tests will never be an adequate substitute for space testing. The principal reason for orbital flight tests of ion engines can be summarized as follows: 1) to test those aspects of engine performance which cannot be simulated on the ground, e.g., the electrical environment of space, zero-gravity behavior, actual launch conditions, micrometeorite bombardment,[26] and long-term ionizer performance in the clean, high-vacuum environment of space; 2) to effect maximum correlation between space and ground tests, such data would permit, wherever possible, the substitution of more economical ground tests for space tests; 3) to develop the reliability of performance and confidence level of ion engines which are necessary prior to the use of electric propulsion in real space missions; and 4) in order to obtain the all-important real experience in the integration problems of ion engines, power systems, and spacecraft.

A list of tests to which the ion thruster is subjected in order to evaluate its performance and life expectancy is presented in Table 1. This table shows the means of conducting such an evaluation in both ground and space tests, together with the preferred test environment for each engine characteristic.

References

[1] Turk, R., "Ion engine supporting research and evaluation," Monthly Progr. Rept., Contract NAS 3-4110, Hughes Research Labs., pp. 11-13 (October 14, 1964).

[2] Becker, J. A., Becker, E. J., and Brandes, R. G., "Reactions of oxygen with pure tungsten and tungsten containing carbon," J. Appl. Phys. **32**, 411–423 (1961).

[3] Andrews, M. R., "The evaporation of thorium from tungsten," Phys. Rev. **33**, 454–458 (1929).

[4] Dushman, S., "Thermionic emission," Rev. Mod. Phys. **2**, 449 (1930).

[5] Ayer, R. B., "Use of thoriated-tungsten filaments in high-power transmitting tubes," Proc. Inst. Radio Engrs. **40**, 591–594 (1952).

[6] Brewer, G. R., Zimmerman, R. L., Berman, D., and King, H. J., "Design criteria and performance of a contact ion engine," AIAA Paper 64-710 (August–September 1964).

[7] Brewer, G. R., "On the nature of leakage currents in cesium contact ion engines," Hughes Research Labs. Research Rept. 281, pp. 40–80 (1963).

[8] Brewer, G. R., "On the nature of leakage currents in cesium contact ion engines," Hughes Research Labs. Research Rept. 281, pp. 7–10 (1963).

[9] Husmann, O. K., "A comparison of the contact ionization of cesium on tungsten with that of molybdenum, tantalum, and rhenium surfaces," AIAA J. **1**, 2607–2614 (1963).

[10] Aamodt, R. L., Brown, L. J., and Nichols, B. D., "Thermionic emission from molybdenum in vapors of cesium and cesium fluoride," J. Appl. Phys. **33**, 2080–2085 (1962); also Wilson, R. G., "Electrode surface physics research," Quart. Rept. 1, Contract NAS 3-5249, Hughes Research Labs. (June 1964); also Quart. Rept. 2 (September 1964).

[11] Brodie, I., "Studies of field emission and electrical breakdown between extended nickel surfaces in vacuum," J. Appl. Phys. **35**, 2324–2332 (1964).

[12] Moore, D. and Forrester, A. T., "Accelerator electrode currents in ion engines," AIAA Paper 64-686 (August–September 1964).

[13] Sellen, J. M. and Kemp, R. F., "Cesium ion beam neutralization in vehicular simulation," ARS Paper 61-84-1778 (June 1961).

[14] Hubach, R. A., "Analytical and experimental studies to develop ion engine ground testing techniques," Final Rept., Contract AF 40-600-948, Hughes Research Labs. (March 1964).

[15] Ward, J. W. and Hubach, R. A., "Neutralization of ion beams from engines of annular geometry," ARS J. **32**, 1730–1731 (1962).

[16] Sellen, J. M. and Cybulski, R. J., "Environmental effects on laboratory and in-flight performance of neutralization systems," AIAA Paper 65-70 (January 1965).

[17] Wilson, R. G., private communication, Hughes Research Labs., Malibu, Calif. (July 1964).

[18] Husmann, O. K., Jamba, D. M., and Denison, D. R., "The influence of the residual gas atmosphere in space chambers on the neutral efflux and the critical temperature of tungsten ionizers," AIAA Paper 64-693 (August–September 1964).

[19] Berman, D., "Correlation of ionizer work function with the residual gas pressures of a vacuum system," Hughes Research Labs., Ion Propulsion Dept., IPD 4-19 (August 1964).

[20] Husmann, O. K., "Ion engine support research and evaluation," Quart. Progr. Rept. 3, pp. 13–15, Contract NAS 3-4110, Hughes Research Labs. (September 1962).

[21] Snouse, T. W., "Sputtering at oblique angles of incidence," NASA TN D-2235 (April 1964).

[22] Molchanov, V. A. and Tel'kovskii, V. G., "Variation of the cathode sputtering coefficients as a function of the angle of incidence of ions on a target," Soviet Phys. **6**, 137–138 (1961).

[23] Wehner, G. K., "Physical sputtering," 1961 Trans. Eighth Vacuum Symp. Second Intern. Congr. (1962).

[24] Magnuson, G. D., "Sputtering mechanisms under ion propulsion conditions," Sixth Quart. Progr. Rept., Contract NAS 8-1592, General Dynamics/Astronautics (1962).

[25] Smith, J. D., "Design, fabrication and testing of a cesium ion rocket engine," Summary Rept., Phase III, Contract NAS 5-517, Hughes Research Labs., pp. 320–373 (March 1964).

[26] Slattery, J. C., "Micrometeorite impact studies," NASA CR-54057, Contract NAS 3-3569, TRW, Inc., Cleveland, Ohio (June 1964).